

Inhibition of cell proliferation, migration and invasion by a glioma-targeted fusion protein combining the p53 C terminus and MDM2-binding domain

Jiawen Yu^{*†‡a}, Meihua Guo^{*a}, Ting Wang^{*}, Xiang Li^{*}, Dan Wang^{*}, Xinying Wang^{*}, Qian Zhang^{*}, Liang Wang^{*}, Yang Zhang^{*}, Chunhui Zhao[‡] and Bin Feng^{*}

^{*}Department of Biotechnology, Dalian Medical University, Dalian 116044, China, [†]Department of Hematology, The First Affiliated Hospital of Dalian Medical University, Dalian 116011, China and [‡]College of Life Sciences, Liaoning Normal University, Dalian 116029, China

Received 30 July 2015; revision accepted 14 October 2015

Abstract

Objectives: The aim of this study was to develop multifunctional fusion proteins for targeting and delivering therapy elements into glioma cells.

Materials and methods: Multifunctional fusion proteins were expressed in *Escherichia coli* and purified using Ni-NTA resin affinity chromatography. Human glioma cells and primary astrocytes were used to analyse their functions. Targeting proteins location to glioma cells was observed by confocal microscopy. Effects of cell viability and proliferation were evaluated using the Cell Counting Kit 8 and colony formation assays. Glioma cell migration and invasion were assessed using transwell assays, and apoptosis was analysed by flow cytometry. In addition, changes in expression of proteins related to the cell cycle and apoptosis were determined by Western blotting.

Results: The protein with highest bioactivity was GL1-riHA2-p53c+m-TAT (GHPc+mT), which combines glioma-targeting peptide GL1 (G), and C terminus (Pc) and mouse double minute domains (Pm) of p53, with the destabilizing lipid membrane peptide riHA2 (H) and cell-penetrating peptide TAT (T). The purified fusion protein was stable in cell culture medium and specifically targeted, and was internalized by, epidermal growth factor receptor (EGFR)-overexpressing glioma cells (U87ΔEGFR). It inhibited cell proliferation, migration and invasion, while flow cytometric analysis

showed increased apoptosis. In addition, GHPc+mT caused significant changes in expression of proteins related to the cell cycle and apoptosis.

Conclusion: GHPc+mT is a multifunctional protein combining targeting, inhibition of glioma cell proliferation and induction of apoptosis, providing some potential to be developed into an effective protein drug delivery system for glioma therapy.

Introduction

Glioblastoma multiforme (GBM) is derived from glial cells and is the most lethal type of primary brain tumour, with annual incidence of six cases per 100 000 (1). GBM is extremely aggressive and due to infiltration and recurrence, there is no treatment option that can permanently remove all the malignant tissue without severely damaging the brain. Treatment includes surgery combined with chemotherapy with agents such as temozolomide (2,3); however, most drugs have limited efficacy as access to the tumour is restricted by the blood–brain barrier. Moreover, median survival of patients is no more than 12 months due to treatment resistance, while survival rate of patients living longer than 5 years is less than 10% after diagnosis (1,4).

Protein transduction therapy is emerging as a promising means of delivering proteins to glioma cells for cancer treatment (5,6). Transcription-transactivating protein (TAT) of human immunodeficiency virus 1 and polyarginine (11R) are the most widely used cell-penetrating peptides (CPPs) for protein transduction into cancer cells (7,8). However, application of CPPs is currently limited by their lack of cell specificity. To this end, glioma-targeting peptides may enhance tumour-anchoring ability; for example, RGD and F3 have been used to target integrin $\alpha v \beta 3$ (9,10), while scorpion

Correspondence: B. Feng, Department of Biotechnology, Dalian Medical University, Dalian 116044, China and C. Zhao, College of Life Sciences, Liaoning Normal University, Dalian 116029, China. Tel.: +86-411-86118844; Fax: +86-411-86118844; E-mails: binfeng@dmu.edu.cn and zch@lnnu.edu.cn

^aThese authors contributed equally to this work.

chlorotoxin, a 36-amino acid peptide, targets matrix metalloproteinase-2 receptor-associated chloride channel, as well as a glioma-specific chloride channel, expressed in membranes of glioma, but not normal, human cells (11). GL1 was first identified to effectively target glioma Gli-a36 cells expressing Δ EGFR cDNA using a peptide phage display library (12). In a previous study by our group, we found that a fusion protein consisting of the 12 amino acid GL1 peptide and EGFP targeted glioma cells with high specificity (13).

The NH₂-terminal 20 amino acid peptide of the influenza virus haemagglutinin-2 protein (riHA2) is pH-sensitive and destabilizes lipid membranes at low pH, to enable the escape of fusion proteins from macropinosomes (14). p53 fusion protein containing HA2 and 11R has been shown to inhibit growth of cancer cells at low concentrations (15). The p53 tumour suppressor regulates transcription of genes such as *p21* and mouse double minute (*MDM2*) that encode proteins involved in cell cycle arrest, DNA repair and apoptosis (16–18). Several peptides derived from p53 have demonstrated anti-proliferative activity (19,20). The C-terminal lysine-rich regulatory domain (amino acids 361–382) is subject to a variety of post-translational modifications (21) and a short peptide derived from this domain (Pc) modulates DNA binding of wild-type p53 *in vitro* and can restore transcriptional transactivation function of some mutant p53 proteins in living cells. Moreover, Pc induces apoptosis in human tumour cell lines of different origins expressing mutant or wild-type p53 protein (22). CPP covalently coupled to a D-isomer peptide of Pc can cause long-term inhibition of bladder cancer growth (23). In addition, a 15-amino acid sequence corresponding to the MDM2 binding site of p53 (Pm) has been shown to modulate proliferation of glioma cells (24), while theranostic protein EC1-Gluc-p53C, generated by combining Pc with ErbB2-targeting peptide EC1 and *Gaussia luciferase* (Gluc), retains target specificity and bioluminescence both *in vitro* and *in vivo* (25).

In the present study, we designed a series of small multifunctional proteins composed of GL1, CPP (TAT), riHA2 and two peptides derived from p53, and evaluated them for their effects on glioma cell proliferation, migration, invasion and apoptosis.

Materials and methods

Cell culture

Two human glioma cell lines paU87 and U87 Δ EGFR (which expresses EGFRvIII) used in this study, were kindly provided by Professor Hideki Matsui of Okayama

University (Okayama, Japan). Cells were cultured in Dulbecco's modified Eagle's medium (DMEM) (Hyclone, Logan, UT, USA) with 10% foetal bovine serum (FBS) and 1% penicillin–streptomycin at 37°C and 5% CO₂. In addition, we used human primary astrocytes (HA) as control glial cells purchased from ScienCell Research Laboratories (ScienCell, San Diego, CA, USA) and maintained in ScienCell astrocytes medium, supplemented with 2% FBS.

Plasmid construction and expression, and purification of fusion proteins

To express *EGFP* and *GL1-EGFP*, the genes were separately amplified from the pEGFP-N1 plasmid (Clontech) using primer sets P1/P2 and P2/P3 (all primer sequences are listed in Table S1). PCR products were purified and digested with the appropriate restriction enzymes and inserted into the pET-22b(+) vector digested with the same enzymes to generate pET-EGFP and pET-GL1-EGFP. To obtain EGFP-TAT and GL1-EGFP-TAT, the genes were separately amplified by reverse PCR with primer set P4/P5, using pET-EGFP and pET-GL1-EGFP as templates.

The pUC-GL1-riHA2-Pc plasmid containing GL1-riHA2-Pc was synthesized by Takara Biotechnology Co., Ltd. (Dalian, China). ZZ (antibody affinity motif of protein A), was inserted in order to increase recombinant protein expression. Factor Xa protease recognition sequence, Ile-Glu-Gly-Arg (IEGR), was inserted after ZZ as a cleavage site. To express ZZ-TAT (abbreviated as ZZ-T), pET-ZZ and pET-GL1-EGFP-TAT, plasmids were digested with *Nde* I and *Eco*R I (Takara) and linked to obtain pET-ZZ-TAT. To express ZZ-IEGR-GL1-riHA2-Pc-TAT (abbreviated as ZZ-GHPcT), ZZ-IEGR-GL1-Pc-TAT (abbreviated as ZZ-GPcT), ZZ-IEGR-GL1-riHA2-TAT (abbreviated as ZZ-GHT), ZZ-IEGR-GL1-Pm-TAT (abbreviated as ZZ-GPmT), ZZ-IEGR-GL1-riHA2-Pm-TAT (abbreviated as ZZ-GHPmT) and ZZ-IEGR-GL1-riHA2-P(c+m)-TAT (abbreviated as ZZ-GHPc+mT), the genes were amplified by reverse PCR with the primer sets P6/P8, P6/P8, P7/P8, P9/P11, P10/P11 and P11/P12, respectively, using pET-ZZ-IEGR-GL1-riHA2-Pc-11R, pET-ZZ-IEGR-GL1-Pc-11R, pET-ZZ-IEGR-GL1-riHA2-11R (previously constructed in our laboratory), pET-ZZ-IEGR-GL1-riHA2-Pc-TAT, pET-ZZ-IEGR-GL1-riHA2-TAT and pET-ZZ-IEGR-GL1-riHA2-Pc-TAT as templates, respectively. All plasmids were verified by 1% agarose gel electrophoresis after double digestion with the above restriction enzymes.

Expression and purification of fusion proteins were carried out as previously described (26). Briefly, expression

plasmids were transformed into *Escherichia coli* BL21 (DE3) and cultured in Luria–Bertani medium containing 100 µg/ml ampicillin at 37°C. When optical density of the culture at 600 nm reached 0.6, recombinant protein expression was induced by adding isopropyl-β-D-thiogalactopyranoside (IPTG) at a final concentration of 0.5 mM at 30°C, overnight. Fusion proteins were purified using a Ni²⁺-His-Bind column (Thermo Scientific, Waltham, MA, USA) and analysed by sodium dodecyl sulphate polyacrylamide gel electrophoresis (SDS-PAGE). Gels were stained with Coomassie Brilliant Blue and Western blotting was used to confirm protein purification with an anti-His (C-terminal) mouse monoclonal antibody (Invitrogen, Carlsbad, CA, USA). Following incubation with horseradish peroxidase-conjugated secondary antibody (TransGen Biotech, Beijing, China), protein bands were visualized employing an enhanced chemiluminescence detection kit (Thermo Scientific) on a ChemiDoc MP imaging system (Bio-Rad, Hercules, CA, USA). Purified proteins were dialysed against phosphate-buffered saline (PBS, pH 7.4) at 4°C for 24 h and stored at -80°C until use.

Purified proteins ZZ-GHPc+mT, ZZ-GHPmT, ZZ-GHPcT and ZZ-GHT were cleaved using protease factor Xa (Promega, Madison, WI, USA) according to the manufacturer's instructions. Cleaved proteins GHPc+mT, GHPmT, GHPcT and GHT were purified using a Ni²⁺-His-Bind column and resolved by 15% SDS-PAGE.

Analysis of specificity and uptake of GL1 and TAT fusion proteins

To evaluate specificity and uptake of fusion proteins containing GL1 and TAT, U87ΔEGFR and paU87 cells were incubated with 2 µM EGFP, GL1-EGFP, EGFP-TAT or GL1-EGFP-TAT for 30 min, then washed twice in PBS and fixed in 4% paraformaldehyde for 10 min followed by incubation with DAPI (Life Technologies, Carlsbad, CA, USA) for 5 min. Fluorescence was visualized by confocal laser microscopy (Leica, Nussloch, Germany) and analysed with Leica Application Suite Advanced Fluorescence software. To test targeting ability of GL1 on primary HA, cells were incubated with 2 µM GL1-EGFP for 30 min, the following treatment being the same as above.

For flow cytometric analysis, cells were incubated with proteins for 2 h as described, washed in pre-cooled PBS, trypsinized and re-suspended, and filtered through a 200-mesh sieve. Gated cells are expressed as percentage of EGFP-positive cells, according to fluorescence intensity. In each analysis, 5 × 10⁶ treated cells were analysed for gated counting.

Cell viability assay

Glioma cells were incubated with 5 µM ZZ-TAT, ZZ-GHPmT, ZZ-GHPcT, ZZ-GPcT, ZZ-GPmT and ZZ-GHPc+mT for 24, 48, 72 and 96 h, and cell viability was analysed using the Cell Counting Kit 8 assay (Dojindo, Tokyo, Japan) according to the manufacturer's instructions. Effects of proteins GHPc+mT, GHPmT, GHPcT and GHT on cell proliferation were evaluated by the same procedure by incubating the cells with fusion proteins (5 µM). Dependence of cell viability on recombinant protein concentration was investigated by incubating cells with protein at concentrations of 1, 2 and 5 µM, and evaluating cell viability at 96 h. To evaluate effects of GHPc+mT on primary HA, cells were incubated with 5 µM GHPc+mT for 24, 48, 72 and 96 h, and cell viability was analysed with the CCK-8 Kit.

Colony formation assay

Cell survival was measured by colony formation assay. U87ΔEGFR and paU87 cells (100, 200 and 500 cells/well) treated with proteins GHPc+mT, GHPmT, GHPcT and GHT (5 µM) for 72 h were seeded in six-well plates (*n* = 3 per group), fixed with methanol, and stained with 2% Giemsa solution. After three washes in PBS, colonies with more than 50 surviving cells were counted using inverted microscope (40× objective). Data are expressed as mean of three experiments for each group.

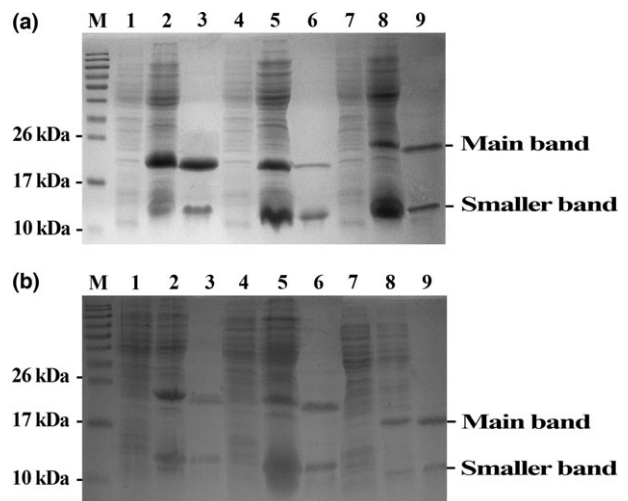


Figure 1. Expression and purification of recombinant proteins. (a) Coomassie Brilliant Blue staining of ZZ-GPcT (lanes 1-3), ZZ-GHT (lanes 4-6) and ZZ-GHPcT (lanes 7-9) resolved by 15% sodium dodecyl sulphate polyacrylamide gel (SDS-PAGE). (b) Coomassie Brilliant Blue staining of ZZ-GPc+mT (lanes 1-3), ZZ-GHPmT (lanes 4-6) and ZZ-GPmT (lanes 7-9) resolved by 15% SDS-PAGE. Lanes 1, 4 and 7 – protein expressions without IPTG induction; lanes 2, 5 and 8 – protein expressions with 0.5 mM IPTG induction; lanes 3, 6 and 9 were purified protein.

Apoptosis assay

After incubating with GHPc+mT, GHPmT, GHPcT and GHT (5 μ M) for 72 h, cells were washed twice in cold PBS and resuspended in cold binding buffer, then treated with annexin V-FITC and propidium iodide for 10 min. Apoptosis was evaluated using a FACS Calibur flow cytometer (BD Biosciences, Franklin Lakes, NJ, USA). Number of annexin V-FITC-positive apoptotic cells was expressed as percentage of total number of cells counted.

Migration and invasion assays

Cells (2×10^5) resuspended in DMEM containing 1% FBS were seeded in chambers containing polycarbonate filters with 8 μ m pores (Corning Inc., Corning, NY, USA). For the invasion assay, upper chambers were prepared with Matrigel (BD Biosciences) according to the manufacturer's protocols. Briefly, inserts were coated with Matrigel at 1:3 dilution and incubated for 30 min, and 3×10^5 cells were resuspended in DMEM containing 1% FBS and plated in the chambers. For all assays, GHPc+mT, GHPmT, GHPcT and GHT (5 μ M) were added to upper and lower chambers and DMEM containing 10% FBS was added to lower chambers as

chemoattractant. After 24 h incubation, cells on upper surfaces of membranes were gently removed using a cotton swab. Cells in the chambers were fixed in methanol and stained with 2% Giemsa solution for 15 min, then washed three times in PBS. Cells in lower chambers and undersides of membranes were counted under an inverted microscope. Values are expressed as mean cell numbers in nine random fields of view (40 \times objective).

Western blotting

After incubating in GHPc+mT, GHPmT, GHPcT and GHT (5 μ M) for 72 h, U87 Δ EGFR cells were collected in RIPA buffer (Sigma, St. Louis, MO, USA). Protein concentration in cell lysates was quantified using a BCA protein assay kit (Multisciences, Hangzhou, China) and then analysed by Western blotting. Blots were probed with primary antibodies against the following proteins: Bcl-2, Bax, E2F-1, phospho-Rb, p21, p53, MDM2 and β -actin (all rabbit polyclonal); CDK4 (mouse monoclonal); and p16 (goat polyclonal). All primary antibodies were purchased from Bioworld Technology, Inc. (St. Louis Park, MN, USA). The following procedures were carried out as above.

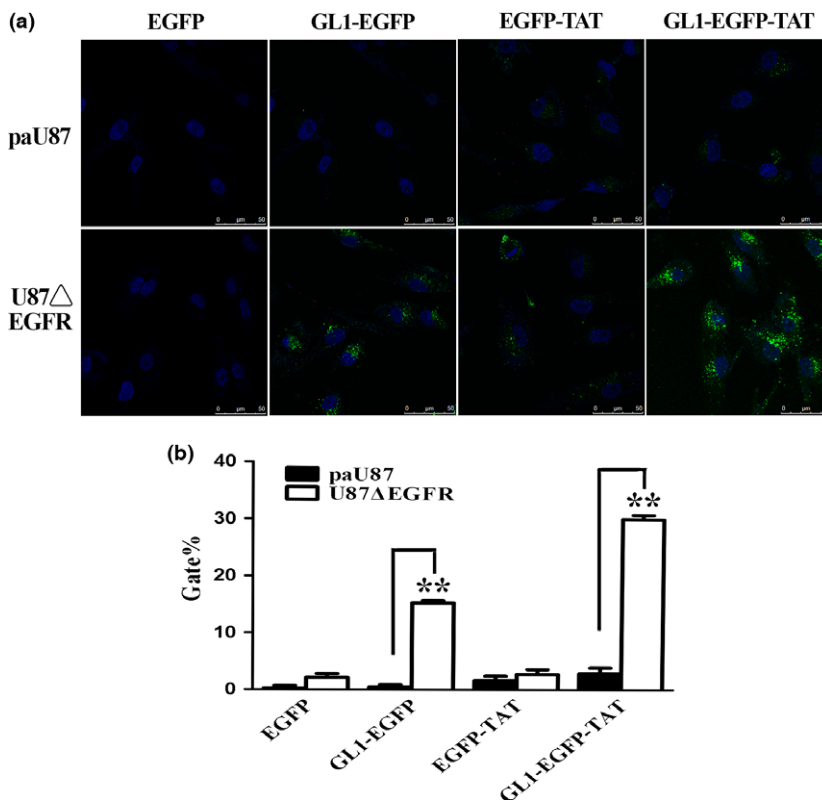


Figure 2. Target specificity and penetration of GLI/TAT fusion proteins. (a,b) EGFP fluorescence in paU87 and U87 Δ EGFR cells treated with fusion proteins. Cells were incubated with 2 μ M EGFP, GLI-EGFP, EGFP-TAT and GLI-EGFP-TAT for 30 min and visualized by confocal microscopy (a) and for 2 h and analysed by flow cytometry (b). Bar = 50 μ m, ** $P < 0.01$.

Statistical analysis

Data are shown as mean \pm SD and were analysed with the Student's *t*-test. $P < 0.05$ was considered statistically significant.

Results

Identification of recombinant proteins

Proteins EGFP (27.7 kDa), GL1-EGFP (29.2 kDa), EGFP-TAT (30.6 kDa), GL1-EGFP-TAT (32.2 kDa), ZZ-TAT (14.5 kDa), ZZ-GHT (19.3 kDa), ZZ-GPcT (19.8 kDa), ZZ-GHPcT (22.0 kDa), ZZ-GHPmT (21.1 kDa), ZZ-GPmT (18.9 kDa) and ZZ-GHPc+mT (24.1 kDa) were expressed, purified and identified by Coomassie Brilliant Blue staining. Additional, smaller molecular weight proteins were also detected, including ZZ-GHT, ZZ-GPcT, ZZ-GHPcT, ZZ-GHPmT, ZZ-GPmT and ZZ-GHPc+mT (Fig. 1a,b). Western blotting analysis showed that the small proteins were recognised by anti-His antibody (Fig. S1). N-terminal sequencing of the small molecular weight protein from ZZ-GHPc+mT showed that its N-terminal five amino acids was the same, with the beginning of ZZ-GHPc+mT.

Functional analysis of fusion protein domains

Compared to EGFP, GL1-EGFP and EGFP-TAT, fusion protein GL1-EGFP-TAT, which combines glioma-targeting peptide GL1 with cell-penetrating peptide TAT, showed higher specificity and penetration in U87 Δ EGFR cells overexpressing mutant EGFR, than in paU87 cells that do not express EGFR (Fig. 2a). The fluorescent signal in GL1-EGFP-TAT-treated U87 Δ EGFR cells was stronger than that in paU87 cells and in cells treated with the other proteins. These

results were confirmed by flow cytometry: after 2 h incubation, gated level reached 30.29% in GL1-EGFP-TAT-treated U87 Δ EGFR cells, compared to levels of 2.06%, 15.32% and 2.76% in U87 Δ EGFR cells treated with EGFP, GL1-EGFP and EGFP-TAT respectively (Fig. 2a). In paU87 cells treated with each of these proteins, gated levels were less than 3%. In HA cells, after treatment with GL1-EGFP, the fluorescent signal could not be observed compared to that of U87 Δ EGFR cells, suggesting GL1 could not target to HA cells (Fig. S2a).

In cell viability analysis, ZZ-fused protein (ZZ-GHPcT) combined with GL1, TAT, Pc and riHA2 had greatest inhibitory effect on U87 Δ EGFR cell prolifera-

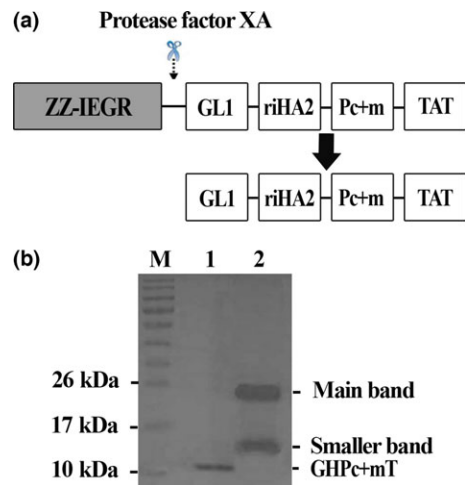


Figure 4. Purification of GHPc+mT. (a) Schema of GHPc+mT purification with the ZZ fusion expression system. The ZZ fraction was cleaved by protease factor Xa from purified ZZ-GHPc+mT, and GHPc+mT was purified with Ni²⁺-His-Bind column. (b) Coomassie Brilliant Blue staining of ZZ-GHPc+mT and purified GHPc+mT in 15% SDS-PAGE. Lane 1, GHPc+mT; lane 2, ZZ-GHPc+mT.

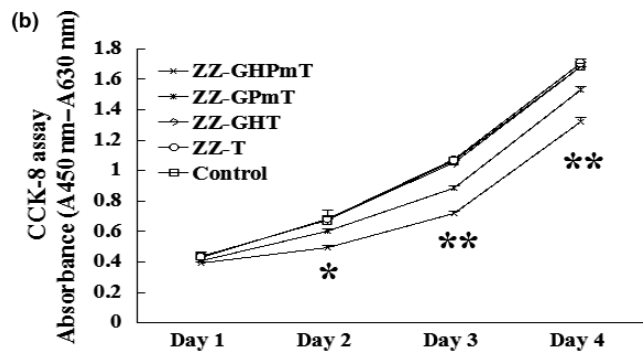
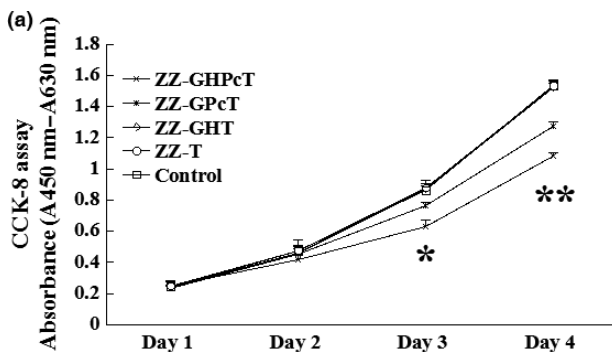


Figure 3. Effect of fusion proteins including p53 C- and N-terminal domain on U87 Δ EGFR cell proliferation. Cells were incubated with 5 μ M ZZ-T, ZZ-GHT, ZZ-GPcT and ZZ-GHPcT containing the C terminus (a) or 5 μ M ZZ-T, ZZ-GHT, ZZ-GPmT and ZZ-GHPmT containing the N-terminal MDM2 domain (b) for the indicated times; cell viability was assessed using a CCK-8 Kit; PBS was used as a control ($n = 6$). * $P < 0.05$, ** $P < 0.01$.

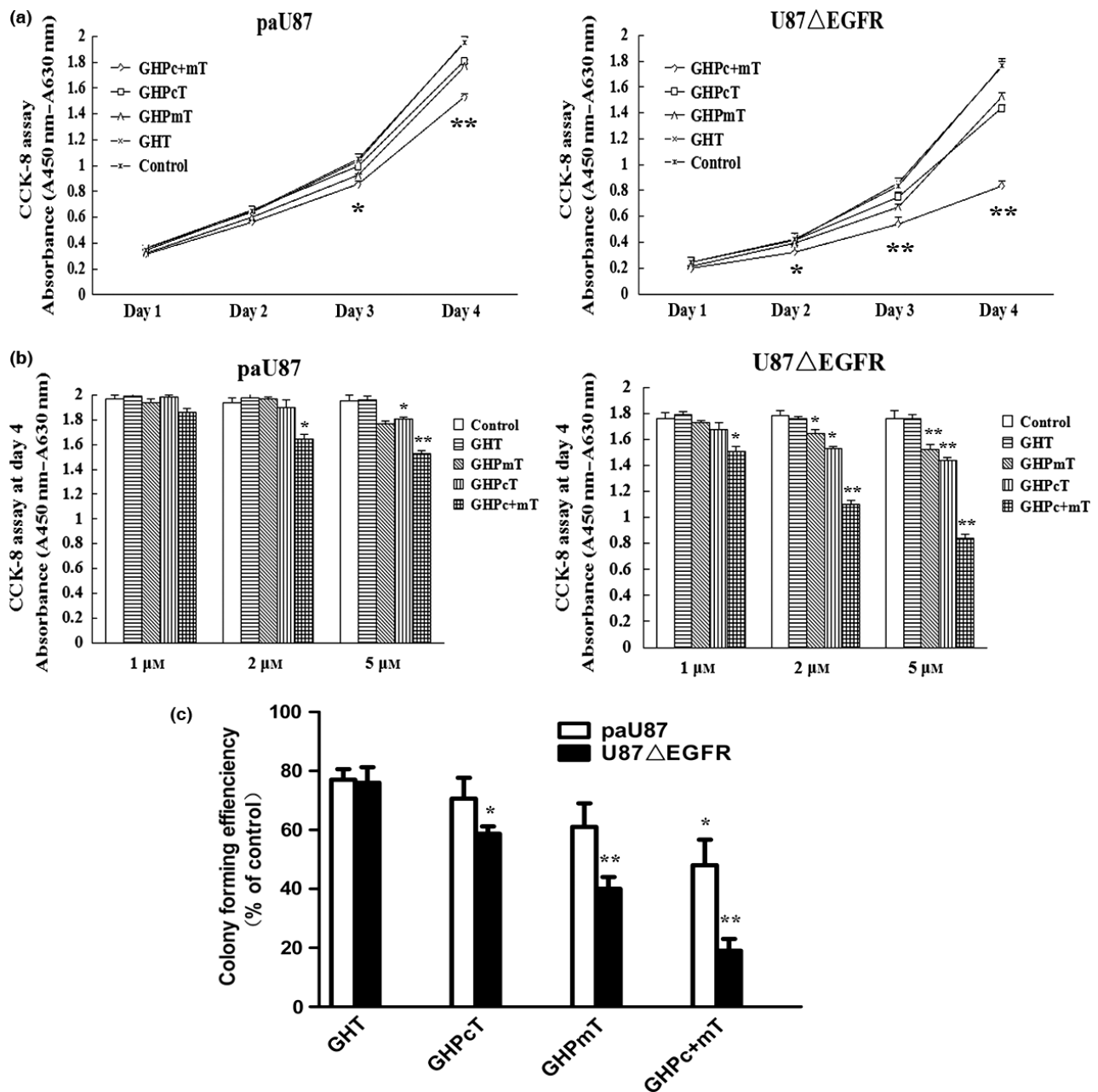


Figure 5. Effect of GHPc+mT on glioma cell proliferation and colony formation. (a) U87ΔEGFR and paU87 cells were incubated with fusion proteins (5 μM) for the indicated times and viability was assessed. (b) Cells were incubated with proteins at different concentrations for 96 h and viability was assessed. (c) Colony formation efficiency after treatment of cells with GHPc+mT; PBS was used as a control ($n = 6$). * $P < 0.05$, ** $P < 0.01$.

tion after 3 and 4 days treatment compared to cells treated with ZZ-T, ZZ-GHT or ZZ-GPcT (Fig. 3a). Similar results were observed in cells treated with ZZ-GHPmT combined with GL1, TAT, Pm and riHA2 (Fig. 3b). GL1, riHA2, TAT and ZZ had no inhibitory effect on cells.

Purification and stability of GHPc+mT

GHPc+mT was cleaved by protease factor Xa from ZZ-GHPc+mT and the purified protein was detected by Coomassie Brilliant Blue staining; its molecular weight is 11.7 kDa (Fig. 4a,b). GHPc+mT, GHPmT, GHPcT and GHT were stable in DMEM as well as in cells incubated

at 37°C, as determined by Western blotting. There was no reduction in signal intensity for any of the proteins up to 72 h in DMEM and 24 h in U87ΔEGFR cells, confirming stability of the fusion proteins (Fig. S3).

GHPc+mT inhibited cell proliferation and colony formation

GHPc+mT containing both Pc and Pm had stronger inhibitory effects on paU87 and U87ΔEGFR cell proliferation than proteins containing either domain alone. paU87 proliferation was suppressed on days 3 and 4, while inhibition of U87ΔEGFR cell proliferation was observed starting from day 2, with an IC₅₀ of 3.98 μM. Inhibition by GHPc+mT was dose-dependent and its level was 52.6% at 5 μM on day 4 for U87ΔEGFR cells (Fig. 5a,b). These results demonstrate that the inhibitory effect was enhanced by combination of Pc and Pm. To HA cells, no obvious inhibition effect was observed from day 2 compared with U87ΔEGFR cells (Fig. S2b).

GHPcT and GHPmT significantly inhibited colony formation in U87ΔEGFR but not paU87 cells; however, GHPc+mT showed the strongest inhibition of colony formation in U87ΔEGFR and paU87 cells compared to GHT-treated control cells (Fig. 5c).

GHPc+mT induced apoptosis

GHPc+mT and GHPcT induced apoptosis of U87ΔEGFR and paU87 cells after 72 h treatment, which

was mainly observed at the early apoptosis time point, by flow cytometric analysis. Increase in levels of apoptosis of GHPc+mT- and GHPcT-treated cells relative to GHT-treated controls was 28.14% and 21.31% in U87ΔEGFR cells respectively; and 24.63% and 10.56% in paU87 cells respectively. Meanwhile, GHPmT had little effect on apoptosis (Fig. 6a).

Expression of apoptosis-related proteins Bcl-2 and Bax were detected by Western blotting. Both Pc and Pm induced up-regulation in level of Bax and down-regulation in that of Bcl-2. GHPc+mT had greater effects than either GHPcT or GHPmT (Fig. 6b).

GHPc+mT inhibited glioma cell migration and invasion

The effect of GHPc+mT on migratory and invasive potentials of glioma cells was evaluated by transwell migration and matrigel invasion assays respectively. Compared to GHT treatment, GHPc+mT significantly reduced U87ΔEGFR cell migration (Fig. 7a,b) and invasion (Fig. 7c,d). In contrast, GHPc+mT and GHPmT inhibited invasion of paU87 cells but had no effect on their migration. These results suggest that Pc+m can inhibit migration and invasion to a greater degree than either Pm or Pc alone.

GHPc+mT modulated expression of cell cycle-related proteins

Expression of cell cycle-related factors was assessed by Western blotting in U87ΔEGFR cells treated with the

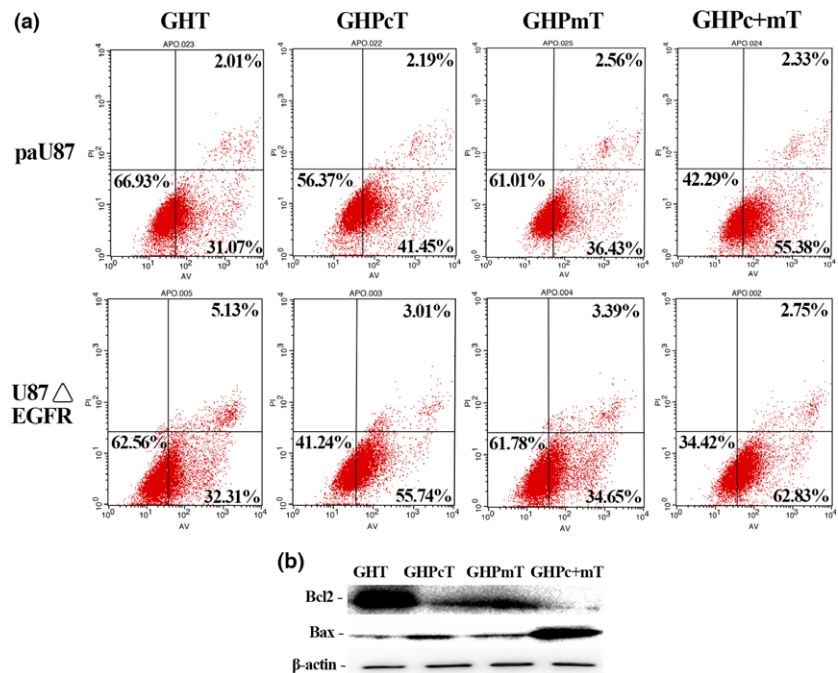


Figure 6. Effect of GHPc+mT on apoptosis. U87ΔEGFR and paU87 cells were incubated with fusion proteins (5 μM) for 72 h and apoptosis was evaluated by flow cytometry (a), while apoptosis-related protein expression was evaluated by Western blotting (b), with β-actin used as a loading control.

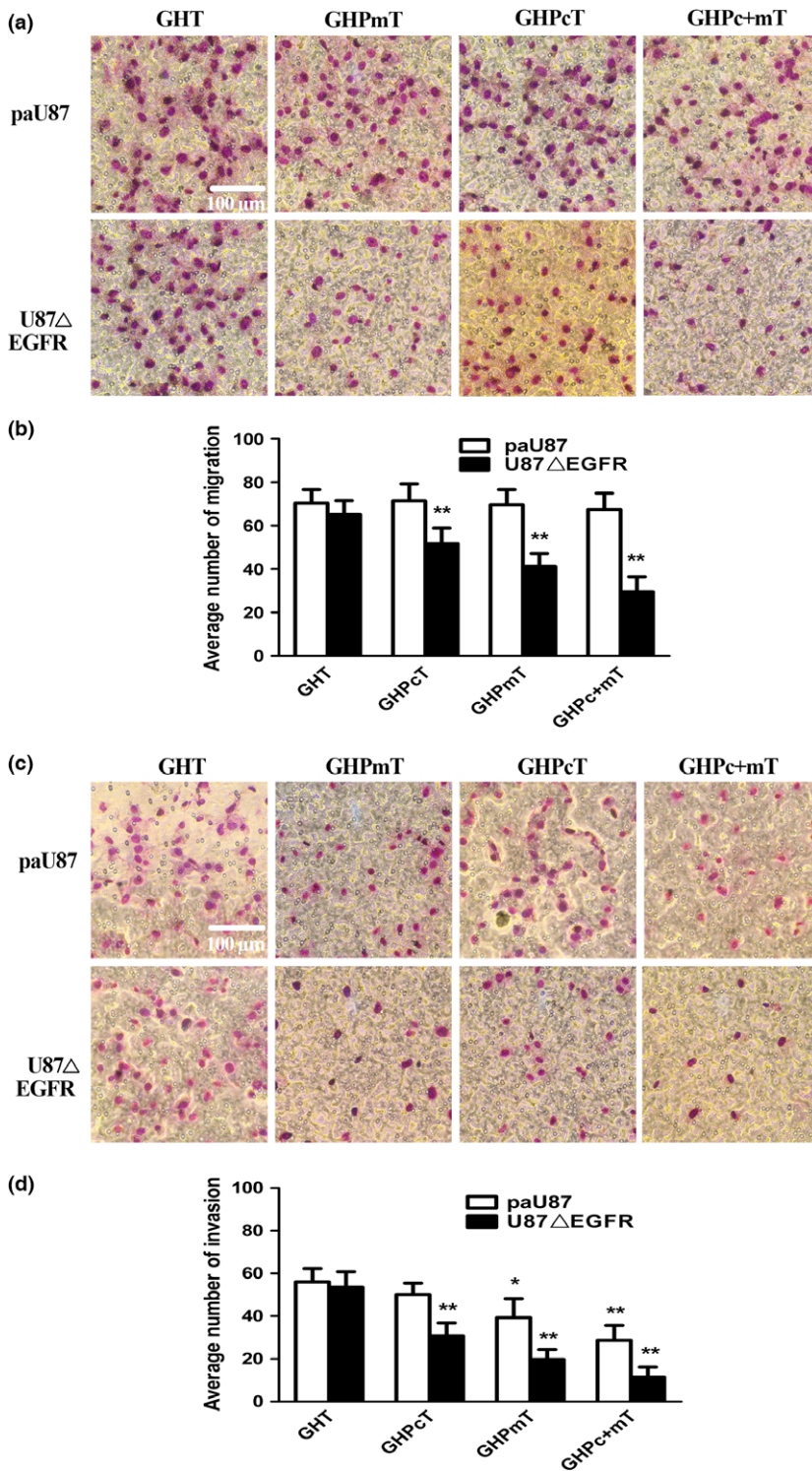


Figure 7. Effect of GHPc+mT on glioma cell migration and invasion. (a) Migration of paU87 and U87ΔEGFR cells treated with the variety of fusion proteins, as determined by transwell migration assay. Bar = 100 μm. (b) Quantitative analysis of A. (c) Invasion of paU87 and U87ΔEGFR cells treated with various fusion proteins, as determined by Matrigel assay. Bar = 100 μm. (d) Quantitative analysis of C. **P* < 0.05, ***P* < 0.01.

variety of fusion proteins. Compared to GHT control, Pc (GHPcT) treatment caused down-regulation in levels of CDK4, phospho-Rb and E2F-1 by increasing p16 expression. Pm (GHPmT) stimulated expression of

CDK4, phospho-Rb and E2F-1 while having no effect on p16 and p21 levels. Meanwhile, GHPc+mT strongly induced up-regulation of p21 and p16 and inhibited CDK4, phospho-Rb and E2F-1 expression (Fig. 8a). Pm

and Pc+m enhanced MDM2 expression, but none of the proteins altered expression of p53 (Fig. 8b).

Discussion

In this study, we constructed multifunctional fusion protein expression vectors, expressed them in *E. coli* and purified them for functional analysis. The ZZ domain was used for fusion as we were able to obtain a high yield for protein ZZ-GLase in a previous study performed by our group (27). Additionally, pET-ZZ expression vector modified by adding IEGR, produced a protein that was efficiently digested by factor Xa. During purification of ZZ fusion proteins, numbers of small molecular weight proteins were also detected. Western blotting analysis revealed that all the small protein bands reacted with the antibody. N-terminal sequencing further confirmed that the small band was ZZ. We therefore concluded that these proteins were produced by early translation termination or resulted from cleavage of full-length fusion proteins in *E. coli*.

EGFR is overexpressed on the surface of GBMs and has been used to target gliomas (28). We found that GL1 fusion proteins had higher affinity for U87 Δ EGFR cells overexpressing EGFR than paU87 cells with no EGFR expression (Fig. S4), suggesting this peptide to have high specificity for EGFR and could therefore be used in a drug delivery system targeting gliomas.

To improve efficiency of protein delivery, we added a cell-penetrating peptide to the fusion proteins. The

multifunctional protein GL1-EGFP-TAT, as shown in Fig. 2, had been demonstrated to penetrate into EGFR overexpressing cells more efficiently than other proteins, with or without any single active peptide. Although 11R confers greater penetration than TAT (29,30), we chose the latter because of its relative ease of purification. TAT-fused proteins tended to aggregate during purification, which precluded their concentration at high concentration; thus, the highest concentration used in this study was 5 μ M. There was no obvious reduction in signal when the proteins were incubated in medium for up to 72 h and for up to 24 h in cells. This stability indicates that GHPc+mT can remain functional over a long period of time after a single administration. GL1 fused to riHA2, Pc, and Pm showed significant bioactivity at this concentration.

It has previously been reported that peptides derived from the p53 C terminus, and the sequence corresponding to the N-terminal MDM2-binding site of p53, can suppress GBM proliferation (23,24). The p53 C-terminal peptide also induces apoptosis in breast cancer cell lines harbouring p53 mutations or overexpressing wild-type p53, but is not found in non-malignant human cell lines expressing wild-type p53 or tumour cells lacking p53, suggesting that peptide activity is p53-dependent (19,22). p53 is stabilized by MDM2-binding peptides in cells expressing wild-type p53 (31,32), and the p53 N-terminal peptide derived from the MDM2-binding site induces necrosis but not apoptosis (20). Although both Pc and Pm altered the expression ratio of Bcl-2 to Bax, results from the flow cytometric analysis showed that the effect of Pc on apoptotic induction differed from that of Pm but was similar to that of Pm+c, suggesting that Pc and Pm act *via* different mechanisms. This was supported by the observations that Pc induced cell cycle arrest, as evidenced by altered levels of p16, CDK4, phospho-Rb and E2F-1. However, Pc and Pc+m blocked the cell cycle at G1/S stage in part *via* up-regulation of p21.

A recent study has suggested that the distinct anti-cancer effects of p53 N- and C-terminal peptides are attributable to differences in their three-dimensional structures. The N-terminal peptide, which has an S-shaped α -helical structure, can disrupt cancer cell membranes in a manner similar to antimicrobial peptides, and thus induce necrosis. In contrast, the C-terminal peptide has a basic α -helical structure that binds to DNA sequences and thereby activates transcription, regulates post-transcriptional modifications and induces apoptosis *via* Fas signalling (33).

Although p53 protein alignment shows no amino acid mutation in both paU87 and U87 Δ EGFR (Fig. S5), superior inhibition effect of GHPm+cT on U87 Δ EGFR suggests that the reason may not be the p53 itself, but the

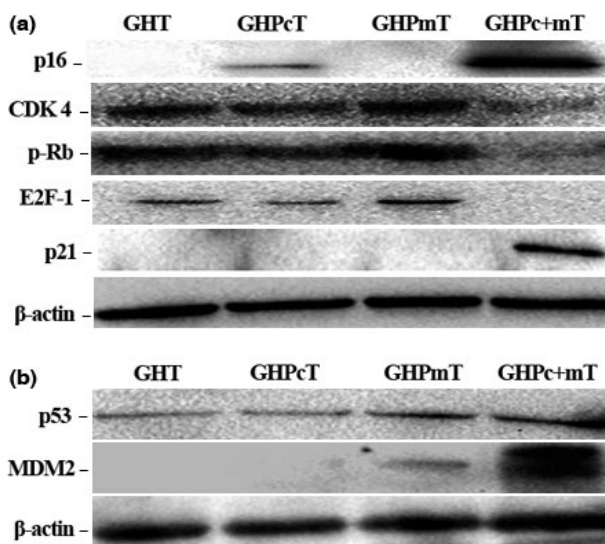


Figure 8. Effect of GHPc+mT on cell cycle-related protein expression. U87 Δ EGFR cells were treated with the variety of fusion proteins and expression levels of cell cycle-related proteins were assessed by Western blotting, with β -actin used as a loading control.

stronger targeting ability to glioma cells or p53-related signalling pathway. The p53 signalling pathway is dysregulated in 87% of GBM cases, with p53 mutations being observed in as many as 30% of them, making p53 an ideal target for glioma treatment (34). Our results demonstrate that the multifunctional protein GHPm+cT can be effectively delivered into glioma cells and enhance the pro-apoptotic function of p53.

Acknowledgements

This work was supported by the National Natural Science Foundation of China (grant nos. 81371676, 81071248 and 21102067).

References

- Gilbert MR, Dignam JJ, Armstrong TS, Wefel JS, Blumenthal DT, Vogelbaum MA *et al.* (2014) A randomized trial of bevacizumab for newly diagnosed glioblastoma. *N. Engl. J. Med.* **370**, 699–708.
- Stupp R, Mason WP, van den Bent MJ, Weller M, Fisher B, Taphoorn MJ *et al.* (2005) Radiotherapy plus concomitant and adjuvant temozolomide for glioblastoma. *N. Engl. J. Med.* **352**, 987–996.
- Grossman SA, Ye X, Piantadosi S, Desideri S, Nabors LB, Rosenfeld M *et al.* (2010) Survival of patients with newly diagnosed glioblastoma treated with radiation and temozolomide in research studies in the United States. *Clin. Cancer Res.* **16**, 2443–2449.
- Krex D, Klink B, Hartmann C, von Deimling A, Pietsch T, Simon M *et al.* (2007) Long-term survival with glioblastoma multiforme. *Brain* **130**, 2596–2606.
- Fonseca SB, Pereira MP, Kelley SO (2009) Recent advances in the use of cell-penetrating peptides for medical and biological applications. *Adv. Drug Deliv. Rev.* **61**, 953–964.
- Heitz F, Morris MC, Divita G (2009) Twenty years of cell-penetrating peptides: from molecular mechanisms to therapeutics. *Br. J. Pharmacol.* **157**, 195–206.
- Gump JM, Dowdy SF (2007) TAT transduction: the molecular mechanism and therapeutic prospects. *Trends Mol. Med.* **13**, 443–448.
- Schmidt N, Mishra A, Lai GH, Wong GC (2010) Arginine-rich cell-penetrating peptides. *FEBS Lett.* **584**, 1806–1813.
- Qin L, Wang CZ, Fan HJ, Zhang CJ, Zhang HW, Lv MH *et al.* (2014) A dual-targeting liposome conjugated with transferrin and arginine-glycine-aspartic acid peptide for glioma-targeting therapy. *Oncol. Lett.* **8**, 2000–2006.
- Hu Q, Gu G, Liu Z, Jiang M, Kang T, Miao D *et al.* (2013) F3 peptide-functionalized PEG-PLA nanoparticles co-administrated with tLyp-1 peptide for anti-glioma drug delivery. *Biomaterials* **34**, 1135–1145.
- Cheng Y, Zhao J, Qiao W, Chen K (2014) Recent advances in diagnosis and treatment of gliomas using chlorotoxin-based bioconjugates. *Am. J. Nucl. Med. Mol. Imaging* **4**, 385–405.
- Ho IA, Hui KM, Lam PY (2010) Isolation of peptide ligands that interact specifically with human glioma cells. *Peptides* **31**, 644–650.
- Yu JW, Guo MH, Zhao CH, Feng B (2012) Prokaryotic expression of GLI-EGFP fusion protein and its targeting of glioma cells. *J. Dalian Med. Univ.* **34**, 428–442.
- Han X, Bushweller JH, Cafiso DS, Tamm LK (2001) Membrane structure and fusion-triggering conformational change of the fusion domain from influenza hemagglutinin. *Nat. Struct. Biol.* **8**, 715–720.
- Michiue H, Tomizawa K, Wei FY, Matsushita M, Lu YF, Ichikawa T *et al.* (2005) The NH2 terminus of influenza virus hemagglutinin-2 subunit peptides enhances the antitumor potency of polyarginine-mediated p53 protein transduction. *J. Biol. Chem.* **280**, 8285–8289.
- Speidel D, Helmbold H, Deppert W (2006) Dissection of transcriptional and non-transcriptional p53 activities in the response to genotoxic stress. *Oncogene* **25**, 940–953.
- Murray-Zmijewski F, Slee EA, Lu X (2008) A complex barcode underlies the heterogeneous response of p53 to stress. *Nat. Rev. Mol. Cell Biol.* **9**, 702–712.
- Lane D, Levine A (2010) p53 Research: the past thirty years and the next thirty years. *Cold Spring Harb. Perspect. Biol.* **2**, a000893.
- Kim AL, Raffo AJ, Brandt-Rauf PW, Pincus MR, Monaco R, Abarzua P *et al.* (1999) Conformational and molecular basis for induction of apoptosis by a p53 C-terminal peptide in human cancer cells. *J. Biol. Chem.* **274**, 34924–34931.
- Do TN, Rosal RV, Drew L, Raffo AJ, Michl J, Pincus MR *et al.* (2003) Preferential induction of necrosis in human breast cancer cells by a p53 peptide derived from the MDM2 binding site. *Oncogene* **22**, 1431–1444.
- Kruse JP, Gu W (2009) Modes of p53 Regulation. *Cell* **137**, 609–622.
- Selivanova G, Iotsova V, Okan I, Fritsche M, Strom M, Groner B *et al.* (1997) Restoration of the growth suppression function of mutant p53 by a synthetic peptide derived from the p53 C-terminal domain. *Nat. Med.* **3**, 632–638.
- Araki D, Takayama K, Inoue M, Watanabe T, Kumon H, Futaki S *et al.* (2010) Cell-penetrating D-isomer peptides of p53 C-terminus: long-term inhibitory effect on the growth of bladder cancer. *Urology* **75**, 813–819.
- Yamada S, Kanno H, Kawahara N (2012) Trans-membrane peptide therapy for malignant glioma by use of a peptide derived from the MDM2 binding site of p53. *J. Neurooncol.* **109**, 7–14.
- Han XJ, Sun LF, Nishiyama Y, Feng B, Michiue H, Seno M *et al.* (2013) Theranostic protein targeting ErbB2 for bioluminescence imaging and therapy for cancer. *PLoS ONE* **8**, e75288.
- Feng B, Zhao CH, Tanaka S, Imanaka H, Imamura K, Nakanishi K (2007) TPR domain of Ser/Thr phosphatase of *Aspergillus oryzae* shows no auto-inhibitory effect on the dephosphorylation activity. *Int. J. Biol. Macromol.* **41**, 281–285.
- Feng B, Tomizawa K, Michiue H, Han XJ, Miyatake S, Matsui H (2010) Development of a bifunctional immunoliposome system for combined drug delivery and imaging in vivo. *Biomaterials* **31**, 4139–4145.
- Roth P, Weller M (2014) Challenges to targeting epidermal growth factor receptor in glioblastoma: escape mechanisms and combinatorial treatment strategies. *Neuro. Oncol.* **16**(Suppl 8), vii–i14–19.
- Matsushita M, Tomizawa K, Moriwaki A, Li ST, Terada H, Matsui H (2001) A high-efficiency protein transduction system demonstrating the role of PKA in long-lasting long-term potentiation. *J. Neurosci.* **21**, 6000–6007.
- Takenobu T, Tomizawa K, Matsushita M, Li ST, Moriwaki A, Lu YF *et al.* (2002) Development of p53 protein transduction therapy using membrane-permeable peptides and the application to oral cancer cells. *Mol. Cancer Ther.* **1**, 1043–1049.

- 31 Bottger A, Bottger V, Sparks A, Liu WL, Howard SF, Lane DP (1997) Design of a synthetic Mdm2-binding mini protein that activates the p53 response in vivo. *Curr. Biol.* **7**, 860–869.
- 32 Wasyluk C, Salvi R, Argentini M, Dureuil C, Delumeau I, Abecassis J *et al.* (1999) p53 mediated death of cells overexpressing MDM2 by an inhibitor of MDM2 interaction with p53. *Oncogene* **18**, 1921–1934.
- 33 Rosal R, Brandt-Rauf P, Pincus MR, Wang H, Mao Y, Li Y *et al.* (2005) The role of alpha-helical structure in p53 peptides as a determinant for their mechanism of cell death: necrosis versus apoptosis. *Adv. Drug Deliv. Rev.* **57**, 653–660.
- 34 The Cancer Genomic Atlas Research Network (2008) Comprehensive genomic characterization defines human glioblastoma genes and core pathways. *Nature* **455**, 1061–1068.
- 35 Corpet F (1988) Multiple sequence alignment with hierarchical clustering. *Nucleic Acids Res.* **16**, 10881–10890.

Supporting Information

Additional Supporting Information may be found in the online version of this article:

Table S1. Primer sequences for expression plasmids.

Fig. S1. Western blotting of purified fusion proteins.

After SDS-PAGE, the purified fusion proteins were transferred to PVDF membrane, the blots were probed with an anti-His mouse monoclonal antibody. Western blotting was performed as described in the Materials and methods section.

Fig. S2. Analysis of GL1-EGFP targeting ability and GHPc+mT inhibiting effect on HA. (a) HA and U87ΔEGFR cells were incubated with 2 μM GL1-EGFP for 30 min, then washed twice in PBS and fixed in 4% paraformaldehyde for 10 min followed by incubation with DAPI for 5 min. Fluorescence was visualized by confocal microscopy. Bar = 50 μm. (b) HA and U87ΔEGFR cells were incubated with 5 μM GHPc+mT for the indicated times and viability was assessed with CCK-8 Kit; PBS was used as a control. ****P < 0.01.**

Fig. S3. Stability of GHPcT, GHPmT, GHT and GHPc+mT in cells and in cell culture medium. (a) Cells were incubated with 5 μM of proteins, after 24 h, they were washed in PBS twice and treated with 0.25% trypsin to remove surface-bound proteins. They were then resuspended in PBS twice before sonication and subjected to Western blotting using an anti-His mouse monoclonal antibody. β-actin was used as loading control. Western blotting was carried out as described in the Materials and methods section. Lanes 1–4 were GHPcT, GHPmT, GHT and GHPc+mT, separately. (b) Proteins incubated with an equal volume of cell culture medium for up to 172 h at 37°C and were analysed at the indicated time points for Western blotting.

Fig. S4. EGFR expression level in different cell lines. Cell lysates of glioma cell lines U87ΔEGFR and paU87 were subjected to 5% SDS-PAGE and transferred to PVDF membranes. Anti-EGFR mouse monoclonal antibody was used for primary antibody. The Western blotting procedure was followed as in the Materials and methods section.

Fig. S5. p53 mutation analysis. Total RNAs of U87ΔEGFR and paU87 were extracted using Trizol reagent (Invitrogen). cDNAs were synthesized by SuperScript II reverse transcriptase (Invitrogen) using the oligo dT primer. p53 cDNAs were amplified using LA Taq DNA polymerase (Takara). The forward and reverse primers for p53 cDNA were 5'-ATGGAGGAGCCGCGAGT CAGATC-3' and 5'-TCAGTCTGAGTCAGGCCCTTCT GTCT-3' respectively. PCR products were ligated with pMD-18T vector and sequenced (performed by TaKaRa Biotechnology). Deduced amino acid sequences were aligned with p53 protein sequence deduced from the conjugation of 11 exons according to the genome sequence (Genbank number NC_000017.11) using the Multalin software (35).